Journal of Molecular Catalysis A: Chemical 423 (2016) 49–60

Contents lists available at ScienceDirect

Journal of Molecular Catalysis A: Chemical

journal homepage: www.elsevier.com/locate/molcata

Cu(II)-amino acid–CaAl-layered double hydroxide complexes, recyclable, efficient catalysts in various oxidative transformations

Gábor Varga[a,b], Szilveszter Ziegenheim[a,b], Szabolcs Muráth[a,b], Zita Csendes[a,b], Ákos Kukovecz[c,d], Zoltán Kónya[c,e], Stefan Carlson[f], László Korecz[g], Erika Varga[h], Péter Pusztai[c], Pál Sipos[b,i], István Pálinkó[a,b,*]

[a] *Department of Organic Chemistry, University of Szeged, Dóm tér 8, Szeged, H-6720 Hungary*
[b] *Materials and Solution Structure Research Group, Institute of Chemistry, University of Szeged, Aradi Vértanúk tere 1, Szeged, H-6720 Hungary*
[c] *Department of Applied and Environmental Chemistry, University of Szeged, Rerrich Béla tér 1, Szeged, H-6720 Hungary*
[d] *MTA-SZTE "Lendület" Porous Nanocomposites Research Group, Rerrich Béla tér 1, Szeged, H-6720 Hungary*
[e] *MTA-SZTE Reaction Kinetics and Surface Chemistry Research Group, Rerrich Béla tér 1, Szeged, H-6720 Hungary*
[f] *Max-IV Laboratory, Lund University, Lund, Sweden*
[g] *Research Center for Natural Sciences, Hungarian Academy of Sciences, P.O. Box 286, Budapest, H-1519 Hungary*
[h] *Department of Inorganic and Analytical Chemistry, University of Szeged, Dóm tér 7, Szeged, H-6720 Hungary*
[i] *Department of Physical Chemistry and Materials Science, University of Szeged, Aradi Vértanúk tere 1, Szeged, H-6720 Hungary*

ARTICLE INFO

Article history:
Received 31 March 2016
Received in revised form 5 June 2016
Accepted 6 June 2016
Available online 13 June 2016

Keywords:
Cu(II)-amino acid complexes in CaAl-LDH
Methods of synthesis
Structural characterization
Catalytic properties in oxidation reactions

ABSTRACT

Intercalated composite materials were prepared with CaAl-layered double hydroxide as host and Cu(II)-amino acid (L-cysteine, L-histidine and L-tyrosine) complex anions as guests. Two methods (intercalation of the ligand first followed by constructing the complex; preforming the complex first, then introducing it among the layers of the host) and optimization of the synthesis conditions were performed to obtain composites having the complex exclusively among the layers. The composite materials were structurally characterized by powder X-ray diffractometry, mid infrared (IR) spectroscopy with ATR (attenuated total reflectance) or photoacoustic detections, transmission and scanning electron microscopies and X-ray photoelectron spectroscopy. Structural features of the intercalant (coordination number, coordination sites) were elucidated by classical chemical and energy dispersive X-ray analyses, EPR (electron paramagnetic spectroscopy), X-ray absorption and far IR spectroscopies. Structural models based on these methods are also given. Catalytic activities, selectivities and recycling abilities of the substances were studied in the oxidation reactions of cyclohexene with peracetic acid and *in situ* formed iodosylbenzene as oxidants in the liquid phase. The catalysts were active in the Ullmann coupling reaction as well. The intercalated substances were found to be efficient and highly selective catalysts with very good recycling abilities.

1. Introduction

Layered double hydroxides (LDHs), because of their relative ease of synthesis, represent inexpensive, versatile and potentially recyclable source of a variety of catalyst supports, catalyst precursors or actual catalysts. LDHs can be found in nature, but for applications they are usually synthesized. They have many representatives, and they have been classified [1]. Part of the hydrotalcite supergroup is the hydrocalumite subgroup – the name giving mineral has the formula of $[Ca_2Al(OH)_6]A \times nH_2O$ – having corrugated brucite-like main layers, which contain ordered arrangements of Ca^{2+} and Al^{3+} or other trivalent ions, seven- and six-coordinated, respectively, in a fixed molar ratio of 2:1. The layers are positively charged, which is compensated by interlayer anions. The anions are exchangeable with more or less difficulties, and even bulkier anions can also be introduced into the interlayer space.

Synthesis of LDHs is most often performed by a wet chemical method: co-precipitation of the LDH from the mixed solution of salt components by NaOH solution; however, mechanochemical routes for their preparation (for a recent original work and an even more recent review, see Refs. [2,3], respectively), occasionally, combined with ultrasound treatment, have been developed and applied [4]. The mechanochemical method worked well in

---

[*] Corresponding author at: Department of Organic Chemistry, University of Szeged, Dóm tér 8, Szeged, H-6720 Hungary.
E-mail address: palinko@chem.u-szeged.hu (I. Pálinkó).

http://dx.doi.org/10.1016/j.molcata.2016.06.008

the preparation of intercalated organic-inorganic host-guest complexes, too [5]. It is to be noted that the intercalated materials to be discussed here were made by the more commonly used direct anion exchange. The host was CaAl-LDH. The guests were Cu(II)-amino acid (L-cysteine, L-histidine and L-tyrosine) complex anions. Synthesis methods were optimized to arrive at composites having the complex exclusively among the layers. The comprehensively characterized organic-inorganic composites were used as catalysts in various oxidation reactions.

Metal complexes have already been incorporated in LDHs, and the early works have been reviewed [6]. Complexes of various transition metal ions (Ni(II), Co(II), Fe(II), Ir(III), Mo(IV, VI), Ru(II), ReO_2(V)) have been incorporated among the layers of LDHs; however, intercalated Cu(II) complex (the ligand was a phthalocyanine macrocycle) appears only once (the original Ref. [7]). Some works have been published since then, but real intercalation was only communicated in two papers [8,9]. The LDH and the ligands in the intercalated complexes were ZnAl-LDH and 2,2-bipyridine-5,5-dicarboxylate [8], and MgAl-LDH and salicylidene-amino acid Schiff base with 1,10-phenanthroline or 2,2′-bipyridine [9]. Catalytic properties of the former intercalated complex were only studied [8]. Oxidation of styrene, ethylbenzene and cyclohexane produced benzaldehyde, acetophenone and a mixture of cyclohexanol and cyclohexanone, respectively, and the catalyst could be used for the second time as well.

However, the ligands have never been amino acids nor the host was CaAl-LDH in any of these works, and in this contribution, a more comprehensive structural characterization of the intercalated system is given than has been performed in the previous studies.

2. Experimental

2.1. Materials and the methods of synthesis

The LDH host containing nitrate anions as charge-compensating anions among the layers were prepared by co-precipitation method. It was synthesized as follows: a mixture of $Ca(NO_3)_2 \times 4H_2O$ (30 mmol) and $Al(NO_3)_3 \times 9H_2O$ (15 mmol) was dissolved in 100 ml of distilled water and was stirred at pH 13 for 12 h. The suspension was filtered and dried for 24 h.

For constructing the Cu-amino acid anions among the layers, two methods were used, similarly to that of the Mn(II)-amino acid anion–CaAl-LDH, published recently [10], and repeated here for the Cu(II)-containing derivatives. In *Method 1*, the amino acid anions were intercalated first, and it was followed by the introduction of the Cu^{2+} anions. In the first step, 2.5×10^{-4} moles of L-cysteine, L-histidine or L-tyrosine were used for the intercalation. The copper ions were introduced in the solution in various amounts (the molar ratio of the amino acid and the copper ions varied from 1:2 to 1:8). In order to identify the optimum conditions, the solvents (aqueous ethanol, aqueous acetone or water) and the pH (from 7.5 to 9.5) were also varied. Designation of composites prepared with *Method 1* will be CaAl–Cu(II)-amino acid anion–LDH. In *Method 2*, the Cu(II)-amino acid complexes were prepared separately applying the same amounts and ratios and varying the solution and the pH in the same way as in *Method 1*. Then, the solution containing the complex was used for the intercalation. Designation of the composites prepared with *Method 2* will be Cu(II)-amino acid anion–CaAl-LDH.

All synthetic operations were performed under N_2 protecting gas to exclude airborne CO_2 reacting with the water content of the LDH forming carbonate ion, which readily intercalates inhibiting the introduction of any other anion.

All the applied compounds were the products of analytical grade from Sigma-Aldrich (Germany), and they were used as received.

2.2. Methods of structural characterisation

X-ray diffraction (XRD) patterns of the fresh and used samples were recorded by a Miniflex II diffractometer (Rigaku, Japan) using $Cu_{K\alpha}$ radiation ($\lambda = 0.15418$ nm) at 40 kV, 30 mA.

The layered structures of the freshly prepared and the used intercalated materials were studied by a TECNAI $G_2$20 X-TWIN transmission electron microscope (TEM, FEI, Germany, 200 kV accelerating voltage).

Morphologies of the pristine and the intercalated samples were investigated using an S-4700 scanning electron microscope (SEM, Hitachi, Japan) with accelerating voltage of 10–18 kV. E(nergy)Dispersion X(-ray) analysis data were obtained with a QX2 energy-dispersive microanalytical system (Röntec, Germany) from two different parts of the sample. The coupled system was applied for providing with elemental maps.

For BET measurements, a NOVA3000 instrument was applied (Quantachrome, USA). The samples were flushed with N_2 at 100 °C for 5 h to clean the surface of any adsorbents.

X-ray absorption measurements (X-ray absorption spectroscopy – XAS) were carried out on the K-edge of copper at beamline I811 of MAXIV-lab (Lund, Sweden). This is a superconducting multipole wiggler beamline equipped with a water-cooled channel cut Si(111) double crystal monochromator delivering at 10 keV, approximately 2×1015 photons/s/0.1% bandwidth with horizontal and vertical FWHM of 7 and 0.3 mrad, respectively. A beam-size of 0.5 mm × 1.0 mm (width × height) was used. The incident beam intensity (I_0) was measured with an ionization chamber filled with a mixture of He/N_2. Higher order harmonics were reduced by detuning the second monochromator to 70% of the maximum intensity. Data collection was performed in the fluorescence mode. The samples were placed in Teflon spacers closed with Kapton tape windows. Data were treated by the EXAFSPAK software package [11].

Combination of three different infrared (IR) techniques was applied for determining the positions of the amino acid anions and/or the anionic forms of the complexes. The instrument for recording the spectra was a Digilab Division FTS-65A/896 FT-IR (BIORAD, USA) spectrophotometer with 4 cm^{-1} resolution. The 4000–600 cm^{-1} wavenumber range was recorded, but the most relevant 1850–600 cm^{-1} range is displayed and discussed. 256 scans were collected for each spectrum. The spectra of each sample were taken in the diffuse reflectance mode (observing both the surface and the bulk of the samples) and using a MTEC 200 photoacoustic (PA) detector (scan speed of 2500 Hz – exploring the composition of the bulk) as well as a single reflection diamond ATR accessory (detecting organic material on the surface of the LDH).

For the identification of Cu–O(S and/or N) vibrations, the far IR spectra were recorded with a Digilab Division FTS-40 (BIORAD, USA) vacuum F(ourier)T(ransfrom)–IR spectrophotometer (4 cm^{-1} resolution, 256 scans). The Nujol mull technique was used between two polyethylene windows (the suspension of 10 mg sample and a drop of Nujol mull).

E(lectron)P(aramagnetic)R(esonance) spectroscopy was used for gathering information on the structure of the complexes. The spectra were recorded with a EleXsys E500 (BRUKER, Germany) spectrometer (microwave frequency 9.51 GHz, microwave power 12 mW, modulation amplitude 5 G, modulation frequency 100 kHz) in quartz EPR tubes at room temperature. Approximately 10 mg of samples were used for each measurement, and their spectra were recorded without any additional sample preparation. All recorded EPR spectra were simulated by an EPR computer program [12].

The amounts of metal ions between the layers were measured by an IRIS Intrepid II ICP-OES (Thermo Fisher Scientific, USA) spectrometer. Before measurements, a few milligrams of the intercalated complexes measured by analytical accuracy were digested

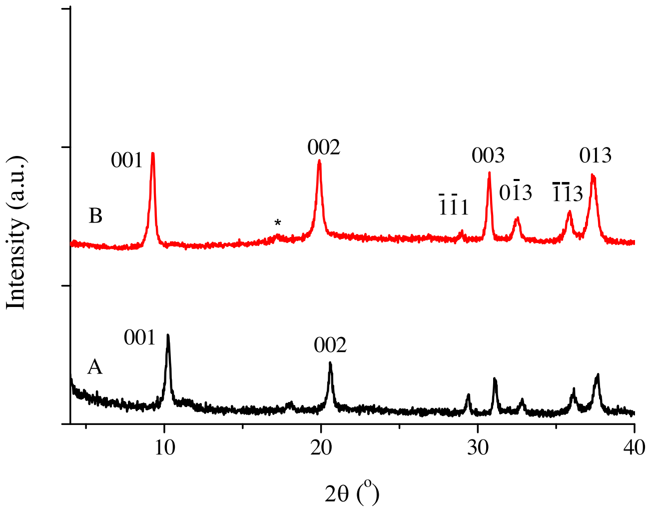

Fig. 1. X-ray diffractograms of A: CaAl-LDH; B: CaAl–Cu(II)-cysteinate–LDH prepared using aqueous ethanol at pH 8 with the nominal ratio of Cu^{2+}: cysteinate = 1:4 (* – trace of $CaCO_3$).

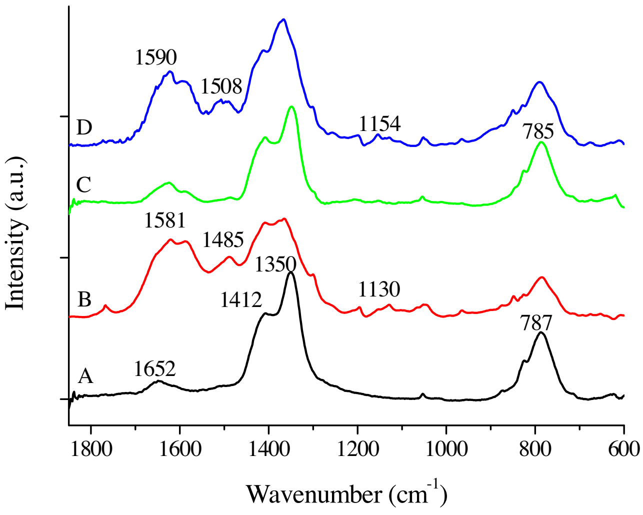

Fig. 2. IR spectra of A: CaAl-LDH (ATR-IR), B: CaAl–Cu(II)-cysteinate–LDH (DRS), C: CaAl–Cu(II)-cysteinate–LDH (ATR-IR), D: CaAl–Cu(II)-cysteinate–LDH (PA-IR).

in 1 cm^3 of cc. H_2SO_4; then, they were diluted with distilled water to 50 cm^3 and filtered. The reaction mixture after filtering the used catalysts was also analyzed for possible leached out metal ions.

UV–vis spectroscopy was used for the quantitative analysis of amino acids at the wavelengths specific for the amino acids measured (L-cysteine: 231 nm, L-histidine: 210.5 nm and L-tyrosine: 273.5 nm). The members of the calibration series as well as the unknown samples were measured on a Shimadzu UV–1650 spectrophotometer.

The X-ray photoelectron spectra (XPS) of the freshly prepared and the used samples were taken with a SPECS instrument equipped with a PHOIBOS 150 MCD 9 hemispherical electron energy analyzer (Germany) operated in the FAT mode. The excitation source was the Kα radiation of magnesium (hν = 1253.6 eV) and aluminum (hν = 1486.3 eV) anodes. The X-ray gun was operated at 180 W power (12 kV, 15 mA). The pass energy was set to 20 eV, the step size was 25 meV, and the collection time in one channel was 150 ms.

2.3. *Catalytic measurements*

Catalytic activities of the intercalated substances were studied in the oxidative transformations of cyclohexene in the liquid phase. In order to find the optimal conditions, the reaction time (1–24 h), the amount of the catalyst (5–45 mg), the reaction temperature (15–55 °C) and the solvents (acetone, ethanol, and dichloromethane) were altered. Furthermore, the oxidants (peracetic acid, (diacetoxy)iodobenzene) were also changed, to establish if it causes significant changes in reaction selectivities (distribution of the products in mol%). The optimum conditions were as follows: 25 mg of catalyst, 10 cm^3 of solvent (acetone when peracetic acid was used; aqueous acetone (5% water, 95% acetone by volume) when (diacetoxy)iodobenzene was used), 5 mmol of cyclohexene, 2.5 mmol of oxidant, 3 h reaction time at 298 K.

Beside cyclohexene, the composites were tested in the Ullmann diaryl etherification reaction [13]. As auxiliary materials, diethyl amine and inorganic bases were applied. Toluene, dimethyl formamide (DMF) or ethanol were tried as solvents, the amount of the catalyst and temperature of the reaction were varied in the 25–45 mg and 298–383 K ranges, respectively. Optimum reaction conditions were identified as follows: 40 mg of catalyst, 5 cm^3 of toluene (when inorganic base was used, it was dissolved in 0.5 cm^3 of water), 0.6 mmol of iodobenzene, 0.5 mmol of phenol, 0.5 mmol of base, 24 h reaction time at 368 K.

At the end of the reactions, the mixtures were analyzed quantitatively by a Hewlett-Packard 5890 Series II gas chromatograph (GC, USA) equipped with flame ionization detector, using an Agilent HP-1 column and the internal standard technique. The temperature was increased in stages from 50 °C to 250 °C. The products were identified *via* using authentic samples.

Conversion as well as turnover frequency (TOF) data are given. The former is defined as the percentage of the reactant consumed and the latter as the number of molecules reacted at one Cu(II) ion in 1 h.

3. Results and discussion

3.1. *The optimisation of the intercalated LDH synthesis*

The major aim of the optimisation was to provide with samples having the Cu-amino acid anionic complexes exclusively among the layers. One may argue that composites having the complexes adsorbed on the outer layer or at both positions can be excellent catalysts. This may be true; however, complexes adsorbed are more prone to leaching during the reactions in the liquid phase than those containing them among the layers exclusively. Moreover, their compositions are less defined as well.

The most important tools, which can be used for checking whether the aim has been achieved or not, are X-ray diffractometry and the comparison of ATR-IR and PA-IR measurements.

If the reflections of the expectedly intercalated LDH are shifted towards lower 2θ values relative to those of pristine LDH (we call the CaAl-LDH samples having nitrate ion among the layers this way), one can be certain that intercalation was successful. However, if the intercalant can be positioned among the layers without increasing the interlayer distance, then the X-ray diffractogram is meaningless in the sense of verifying intercalation. Nevertheless, PA-IR measurement is capable of indicating the presence of the guest material even in this case, while ATR-IR can detect whether it is present on the outer surface or not.

3.1.1. *Cu(II)-cysteinate containing samples*

Method 1 proved to be successful in preparing the desired host-guest complex. Aqueous ethanol (5/95 vol% composition) and a 1:4 nominal molar ratio of copper(II) and cysteinate had to be used in

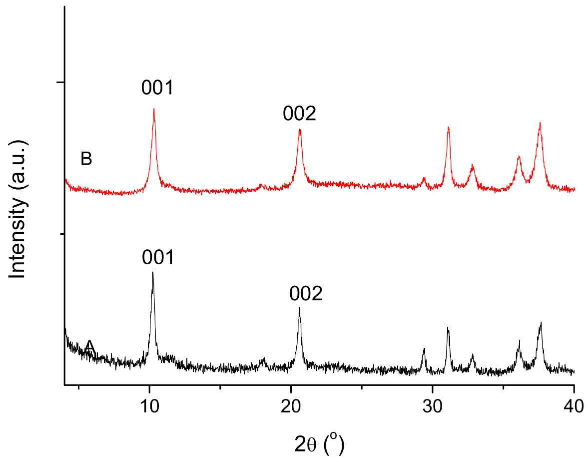

Fig. 3. X-ray diffractograms of A: CaAl-LDH; B: Cu(II)-histidinate–CaAl-LDH prepared using aqueous ethanol at pH 8 with the nominal ratio of Cu^{2+} : histidinate = 1:4.

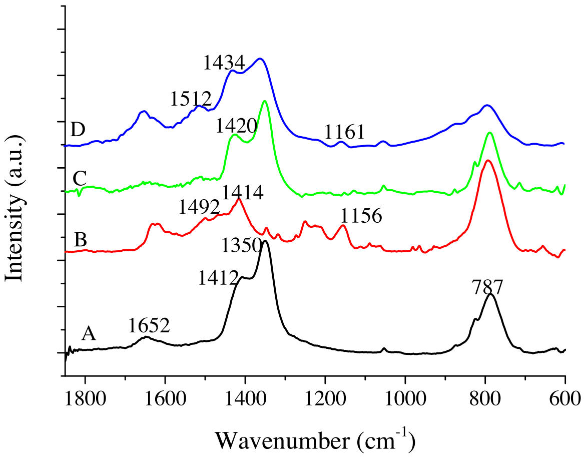

Fig. 4. IR spectra of A: CaAl-LDH (ATR-IR), B: Cu(II)-histidinate–CaAl-LDH (DRS), C: Cu(II)-histidinate–CaAl-LDH (ATR-IR), D: Cu(II)-histidinate–CaAl-LDH (PA-IR).

the synthesis. In the diffractogram (Fig. 1) the shifts of both the 001 and 002 reflections towards lower 2Θ values are observed. The interlayer spacing (the interlayer distance plus the thickness of a layer) increased from 0.857 nm to 0.949 nm as the result of intercalation.

The comparison of the ATR-IR spectrum of the pristine LDH (Fig. 2, trace A) and that of the composite sample (Fig. 2, trace C) revealed that there was no organic material on the outer surface. The two carboxylate vibrations in the PA-IR spectra at 1590 and 1508 cm^{-1} attest the presence of the organic material.

Quantitative analysis of the composite revealed that Cu^{2+} was also present and the actual copper to cysteinate ions was close to 1:2 (Table 1, row 2).

3.1.2. Cu(II)-histidinate containing samples

Here, the sample prepared by *Method 2* met the aims of the synthesis. Although the 001 and 002 reflections practically remained at the same position for the intercalated sample as for the pristine LDH (the interlayer distance remained 0.857 nm) (Fig. 3), the PA-IR spectrum indicated the presence of the organic material in the LDH (Fig. 4, trace D). The ATR-IR spectrum of the intercalated sample did not display the vibrations of the amino acid (Fig. 4, trace C); therefore, it can safely be stated that all the amino acid anions reside among the layers of the LDH. The optimum synthesis conditions are as follows: aqueous ethanol as the solvent, pH 8, nominal ratio of Cu^{2+}:histidinate = 1:4.

The chemical analysis of the sample prepared revealed that the actual Cu^{2+}: histidinate ratio was 1:2 (Table 1, row 3). The unchanged interlayer spacing indicate that the complex was accommodated between the layers in a way, which does not require layer expansion.

3.1.3. Cu(II)-tyrosinate containing samples

Again, *Method 2* provided with the desired composite material. The optimum conditions were the same as for Cu(II)-histidinate–CaAl-LDH: aqueous ethanol as the solvent, pH 8, nominal ratio of Cu^{2+}:tyrosinate = 1:4. During the introduction of the pre-prepared complex, partial intercalation only occurred. The reflections of the pristine LDH are also seen in the diffractogram (Fig. 5, trace B). The reflections related to the intercalated material shifted towards lower angles; it means that the interlayer distance of LDH increased from 0.857 nm to 1.110 nm.

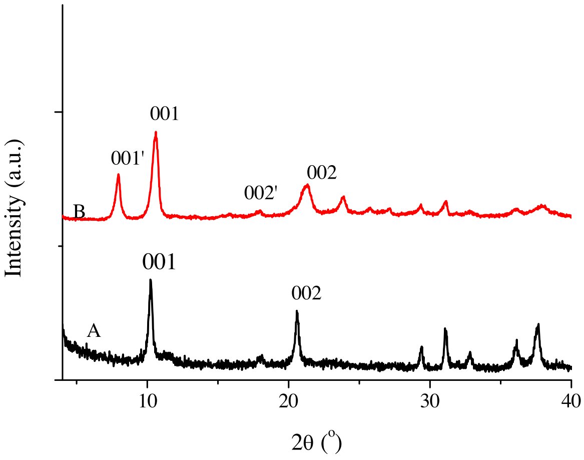

Fig. 5. X-ray diffractograms of A: CaAl-LDH; B: Cu(II)-tyrosinate–CaAl-LDH prepared using aqueous ethanol at pH 8 with the nominal ratio of Cu^{2+}: tyrosinate = 1:4.

The ATR-IR spectrum did not indicate organic material on the outer surface of the LDH, while the PA-IR spectrum displayed vibrations of the organic material as the sign of its presence in the bulk of the LDH (Fig. 6).

Analytical measurement performed on the intercalated sample revealed a Cu^{2+}:tyrosinate ratio close to 2. (Table 1, row 4).

3.2. Studying the intercalated samples with XPS

XPS measurements were able to show both the chemical identities and the oxidation states of the constituents of the intercalated systems. As an example, the spectrum of the Cu^{2+} ions in Cu(II)-histidinate–CaAl-LDH is shown in Fig. 7.

Table 1
Quantitative analytical data of the intercalant in the selected composite LDHs together with BET data.

Composite	Amino acid (mol/0.3 g LDH)	Cu(II) (mol/0.3 g LDH)	Amino acid/Cu(II)	BET surface area (m^2/g)
CaAl–Cu(II)-Cys–LDH	2.5×10^{-4}	1.2×10^{-4}	2.1	61.7
Cu(II)-His-CaAl-LDH	2.2×10^{-4}	1.1×10^{-4}	2.0	59.8
Cu(II)-Tyr–CaAl-LDH	3.8×10^{-4}	1.8×10^{-4}	2.1	60.9

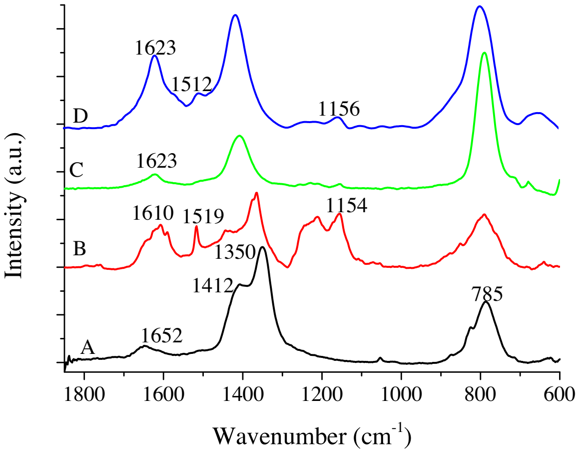

Fig. 6. IR spectra of A: CaAl-LDH (ATR-IR), B: Cu(II)-tyrosinate–CaAl-LDH (DRS), C: Cu(II)-tyrosinate–CaAl-LDH (ATR-IR); D: Cu(II)-tyrosinate–CaAl-LDH (PA-IR).

The other spectra relevant to the other building blocks of the intercalated system are shown in SFigs. 1–5 (Figure in the Supplementary Material is designated as SFig.).

3.3. TEM and SEM images of the intercalated samples

Visualization of the layered structure is possible by TEM measurements. Nevertheless, obtaining the image is not easy, one needs to have properly positioned particles and the high-energy electron beam can easily damage the composite materials. After several trials we could take the images and here, that of the CaAl–Cu(II)-cysteinate–LDH sample is shown (Fig. 8). Those of the other composites are displayed in SFigs. 6 and 7.

SEM provide information about the morphologies of the samples. In all instances, the regular LDH-like morphology, platelets of close to hexagonal shape, is recognizable (Fig. 9).

As an example, SEM–EDX elemental map of the CaAl–Cu(II)-cysteinate–LDH sample is displayed in Fig. 10. It shows the presence of sulphur and copper in the cysteinate-containing sample. Copper and sulphur are seen in the picture, evenly distributed.

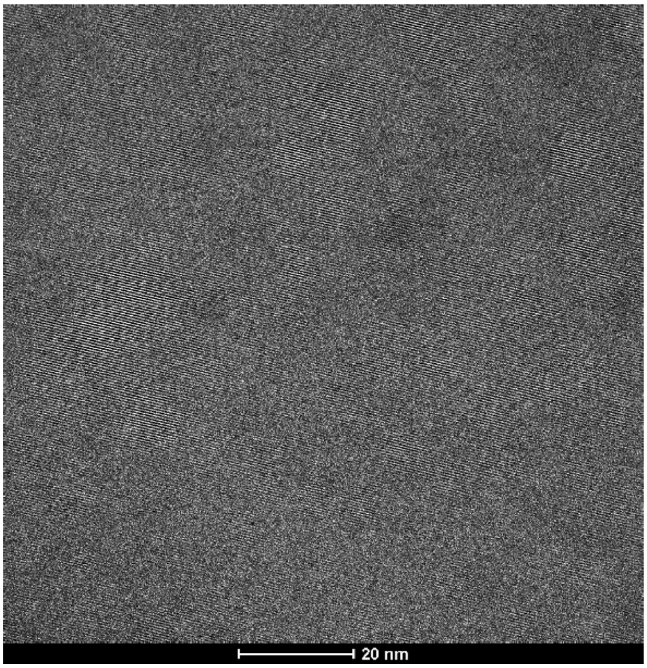

Fig. 8. TEM image of the as-prepared the CaAl–Cu(II)-cysteinate–LDH sample.

3.4. Characterization of the intercalated complexes

Information on the coordination number and the coordinating atoms/groups of the intercalated complexes can be acquired through the combination of information derived from far IR, ESR and X-ray absorption spectroscopies.

Much information is expected from the X-ray absorption spectra (Figs. 11 and 12).

The position of the edge verifies the presence of Cu^{2+} in system. The near edge (X-ray near edge structure – XANES) region gives the coordination number, which was six for all three samples. The extended (extended X-ray absorption fine structure – EXAFS) region provides with bond distances. If a good model is found in terms of coordination number, coordinating atoms (*i.e.*, bond

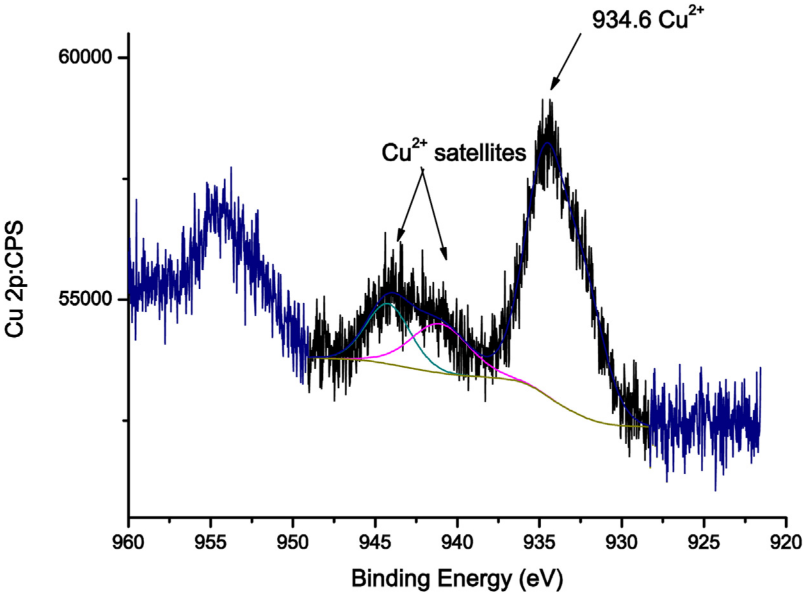

Fig. 7. XPS showing the Cu^{2+} content of the as-prepared Cu(II)-histidinate–CaAl-LDH.

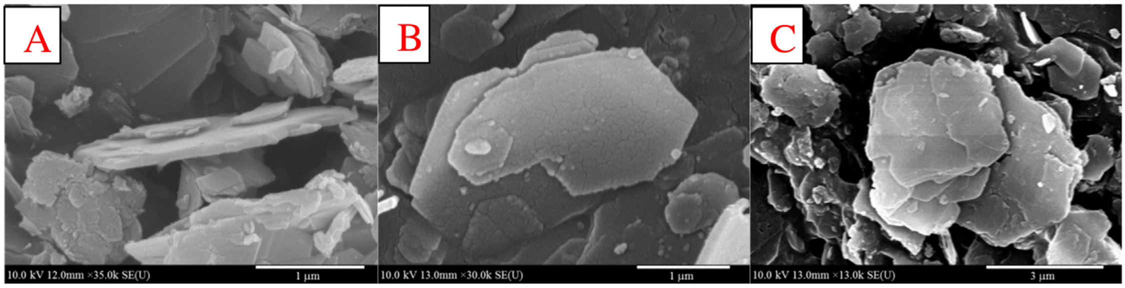

Fig. 9. The SEM images of the (a) CaAl–Cu(II)-cysteinate–LDH, (b) Cu(II)-histidinate–CaAl-LDH and (c) Cu(II)-tyrosinate–CaAl-LDH samples.

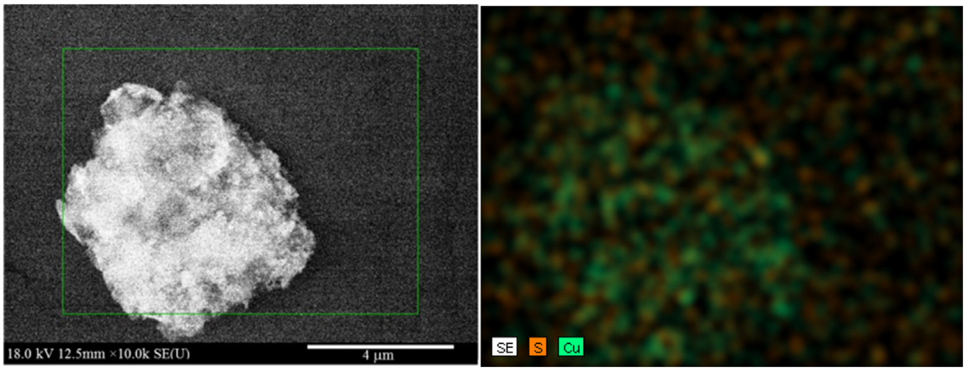

Fig. 10. The SEM–EDX elemental map of the CaAl–Cu(II)-cysteinate–LDH sample.

Table 2
Parameters calculated from the fitted EXAFS spectra (N: coordination number, R: bond length, σ^2 Debye-Waller factor, F-factor: goodness of fit).

Composites	Cu(II)–X	N	R (Å)	σ^2 (Å^2)	F factor (%)
CaAl–Cu(II)-cysteinate–LDH	N/O	2	2.009	0.005350	3.86
	S	2	1.969	0.89470	
	N/O	2	2.123	0.005130	
Cu(II)-histidinate–CaAl-LDH	N/O	4	1.939	0.006860	8.10
	N/O	2	2.330	0.012750	
Cu(II)-tyrosinate–CaAl-LDH	N/O	4	1.949	0.004416	7.73
	N/O	2	2.290	0.004651	

Table 3
EPR parameters of the two selected intercalated samples.

CaAl-LDH sample	g_x	g_y	g_z	A_{Cux} (G)	A_{Cuy} (G)	A_{Cuz} (G)	A_{Nx} (G)	A_{Ny} (G)	A_{Nz} (G)
Cu(II)-His[a]	2.042549	2.06859	2.323077	18.95	19.42	123.14	27.65	26.45	21.46
Cu(II)-Cys[b]	2.046638	2.06004	2.247786	11.30	15.89	160.78	11.11	7.49	20.81

[a] and [b] – for the goodness of fit R = 0.9964 and 0.9816, respectively.

distances), an acceptable F factor (smaller than 20%) is obtained. Table 2 contains all these data, and it is clear that the models constructed are suitable to describe the local structure of Cu(II) in the complexes.

Unfortunately, from these data the N and O coordination cannot be distinghuised; nevertheless, it is seen that the best fit was achieved when two different bond lengths were included in the model. It may be due to Jahn–Teller distortion as was detected in former works [14,15]. However, it is clear that the sulphur atom of the cysteinate ligand takes place in the coordination.

Far IR spectra may reveal metal–functional group vibrations directly. Indeed, spectra B–D in Fig. 13 reveal a band around 390 cm^{-1}, not seen in the spectrum of the pristine LDH (spectrum A). This band can be attributed to the vibration of the coordinated amino group [16]. Another new band is evident at 227 cm^{-1}, but only in the spectrum of Cu(II)-histidinate–CaAl-LDH. Therefore, and on the basis of the observations in Ref. [16], it is assigned to copper–imidazolate nitrogen vibration. Unfortunately, the possible copper–carboxylate oxygen vibration overlaps with that of the pristine LDH at 287 cm^{-1}, and thus, it cannot be resolved.

In Fig. 14 the EPR spectra of the Cu(II)-histidinate–CaAl-LDH and the CaAl–Cu(II)-cysteinate–LDH are displayed. That of the Cu(II)-tyrosinate–CaAl-LDH was also registered (SFig. 8); however, it lacks the hyperfine structure, therefore, it is disclosed from further discussion. The recorded EPR spectra are anisotropic, similar to spectra, which can be obtained at low-temperature. The only characteristic difference that the resolution is lower than for the common low-temperature copper complex system.

Data relevant to the Cu^{2+} ion ligand interactions are listed in Table 3. The precision of the evaluation of $\mathbf{g}_x$, $\mathbf{g}_y$, $\mathbf{A}_{Cux}$ and $\mathbf{A}_{Cuz}$ are relatively low, since the systems do not show Cu hyperfine splitting in the direction of x and y due to the broad lines. Since the values of the g tensor are close to the axial symmetry ones, a distorted octahedral geometry elongated along the fourfold symmetry Z-axis with some rhombic distortion can be assumed around the copper ion [17].

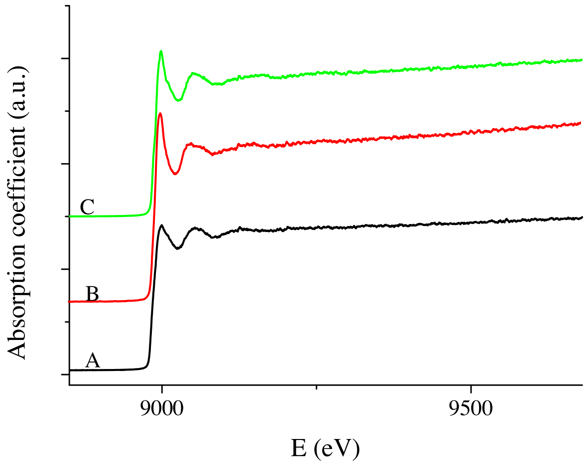

Fig. 11. Cu-K-edge X-ray absorption spectra of A: CaAl–Cu(II)-cysteinate–LDH, B: Cu(II)-histidinate–CaAl-LDH and C: Cu(II)-tyrosinate–CaAl-LDH.

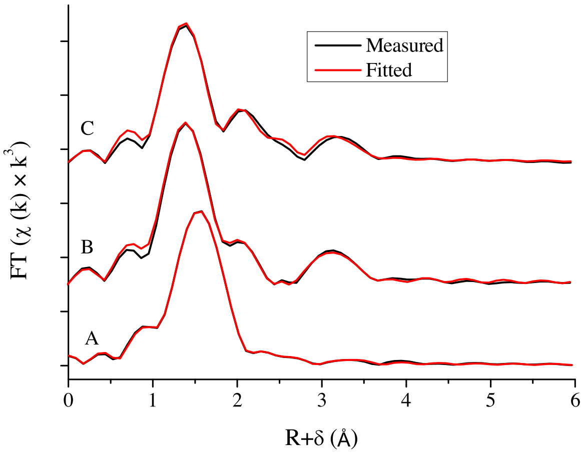

Fig. 12. Observed and fitted Cu(II)-K-edge radial distribution functions of A: CaAl–Cu(II)-cysteinate–LDH, B: Cu(II)-histidinate–CaAl-LDH and C: Cu(II)-tyrosinate–CaAl-LDH.

For the case of Cu(II)-histidinate–CaAl-LDH system, the number of coordinated N can be evaluated from the N splitting (shoulders in the "perpendicular" line). Three nitrogens are coordinated to the Cu^{2+} ion, an $N_{imidazole}N_{amino}N_{amino}O_{carboxylate}$ coordination environment in tetragonal arrangement around the Cu^{2+} ion can be expected. The fifth and sixth positions are probably filled by water molecules coordinated through their oxygen atoms [18,19]. For the cysteinate-containing material the values of the above parameters indicate $N_{amino}N_{amino}S_{thiolate}S_{thiolate}$ tetragonally-shaped coordination environment [20,21] with two molecules of water coordinated through their oxygen atoms in the fifth and sixth position.

3.5. Models of the intercalated copper-amino acid complexes

Unifying the various pieces of information obtained by analytical and structural characterisation methods complementing with chemical common sense, the following picture emerges for the intercalated complexes. The complexes have elongated octahedral coordination geometry (XAS, EPR). The copper ion is surrounded by two amino acid anions (quantitative analysis – ICP-OES, UV–vis), which are coordinated as bidentate ligands in tetragonal arrangement (XAS, EPR). The fifth and sixth positions are probably filled with water molecules (XAS). The amino groups are always coordinated through the nitrogen atom (far IR, EPR). The imidazolate nitrogen and the amino nitrogen of one of the histidinate ligands and the amino nitrogen and the carboxylate oxygen of the other one are coordinated (far IR, EPR). The remaining carboxylate ion and the deprotonated imidazole nitrogens keep the complex among the layers of the LDH. The sulphur atoms in the thiolate groups of both cysteinate ligands are coordinating atom (XAS, EPR). In the tyrosinate-containing composite, the amino nitrogens as well as the carboxylate oxygens are coordinated (XAS, chemical common sense). The phenolate ions keep the complex among the layers of the LDH. The amino nitrogens and the phenolate oxygens cannot coordinate at the same time because of steric reasons.

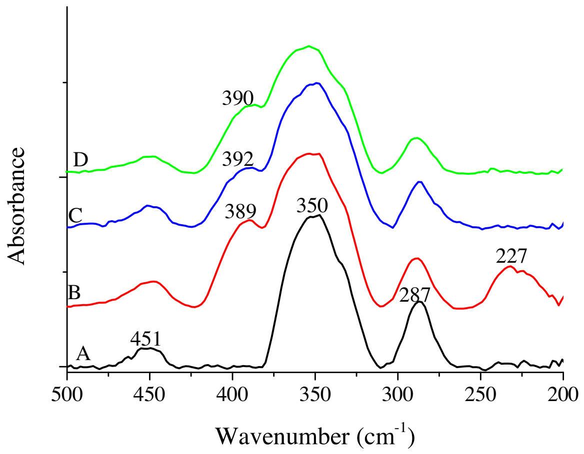

Fig. 13. Far IR spectra of A: CaAl-LDH, B: Cu(II)-histidinate–CaAl-LDH, C: CaAl–Cu(II)-cysteinate–LDH, D: Cu(II)-tyrosinate–CaAl-LDH.

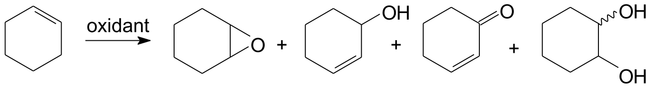

Scheme 1. The oxidative transformations of cyclohexene.

On the basis of the above-reasoning, using the data obtained from X-ray absorption measurements and knowing that the thickness of the layer is 0.234 nm [22] and the interlayer distances from XRD measurements, approximate models can be put together for the composites, mainly to help visualisation (Fig. 15).

3.6. Catalytic properties of the composites

3.6.1. Cyclohexene oxidations using two different oxidants

Oxidation reactions of functional groups, like e.g. alcoholic hydroxide [23] or carbon–carbon double bonds are frequently used probe reactions to test various catalyst preparations [24].

First, the composites were used in the oxidative transformations of cyclohexene (Scheme 1). Two different oxidants were used in these reactions, and significant differences were experienced in the rate of the transformations and product distributions.

Peracetic acid was one of the oxidants. Conversion, turnover frequency (TOF – no. of transformed molecules over one Cu^{2+} ion per hour) and selectivity (mol%) data are summarized in Table 4. H_2O_2 was also tried; however, it was decomposed over the composites.

Acetone was the solvent of choice, because the rate of the decomposition of peracetic acid in acetone is very slow [25]. It was checked experimentally; our composites did not decompose peracetic acid under the experimental conditions used for the oxidative transformations of cyclohexene. Peracetic acid alone (without catalyst) was able to transform the cyclohexene; however, both the conversion and the epoxide selectivity were significantly lower than in the presence of the composites. It is especially true regarding selectivities: the composites were found to be extremely

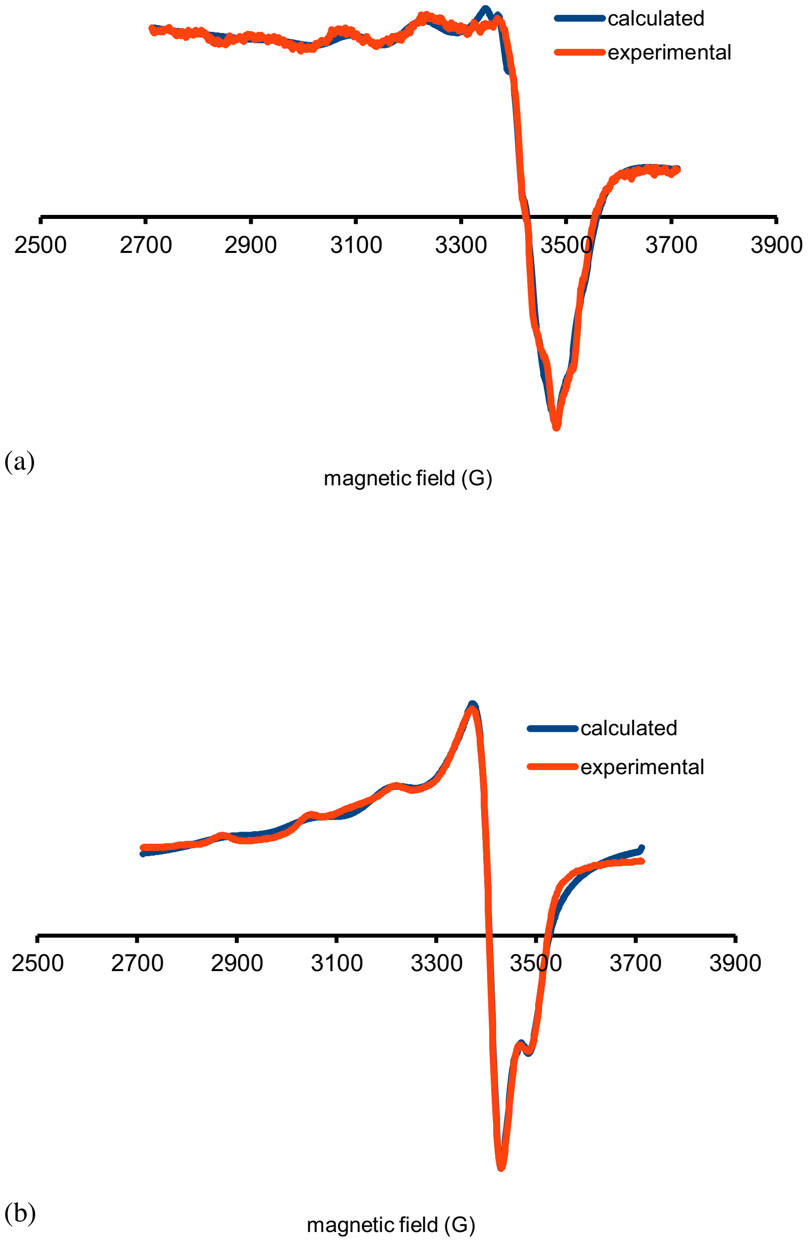

Fig. 14. EPR spectra of (a) Cu(II)-histidinate–CaAl-LDH, (b) CaAl–Cu(II)-cysteinate–LDH.

Table 4
The TOF/conversion and selectivity results of the oxidation of cyclohexene after 4 h (catalyst: 35 mg, acetone: 10 cm^3, cyclohexene: 5 mmol, peracetic acid: 2.5 mmol, temperature: 298 K).

Catalyst	TOF (1/h)/Conversion (%)	Epoxide (%)	2-Chex-1-ol (%)	2-Chex-1-one (%)	*trans* diol (%)
–	nr/21	64	4	2	30
CaAl-LDH	nr/18	63	4	5	28
CaAl–Cu(II)-Cys–LDH	20.1/47	100	0	0	0
Cu(II)-His–CaAl-LDH	20.5/42	98	0	0	2
Cu(II)-Tyr–CaAl-LDH	13.8/49	97	0	1	2

selective epoxidation catalysts. Activity of the pristine LDH was also checked; the obtained conversion and selectivity data were basically the same as they were in the homogeneous reaction. The recycling abilities of the composites are also noteworthy; only slight deactivation was experienced even in the fourth run (Table 5). No special reactivation was required between the runs; the catalysts were only rinsed with acetone.

Acetic acid formed upon the decomposition peracetic acid was probably adsorbed over the outer surface of the LDH being of basic character; therefore, it could not initiate epoxide ring opening. This may be behind the very high epoxide selectivity.

The process became diol-selective when diacetoxy iodobenzene was used as the precursor of the real oxidant. This compound was

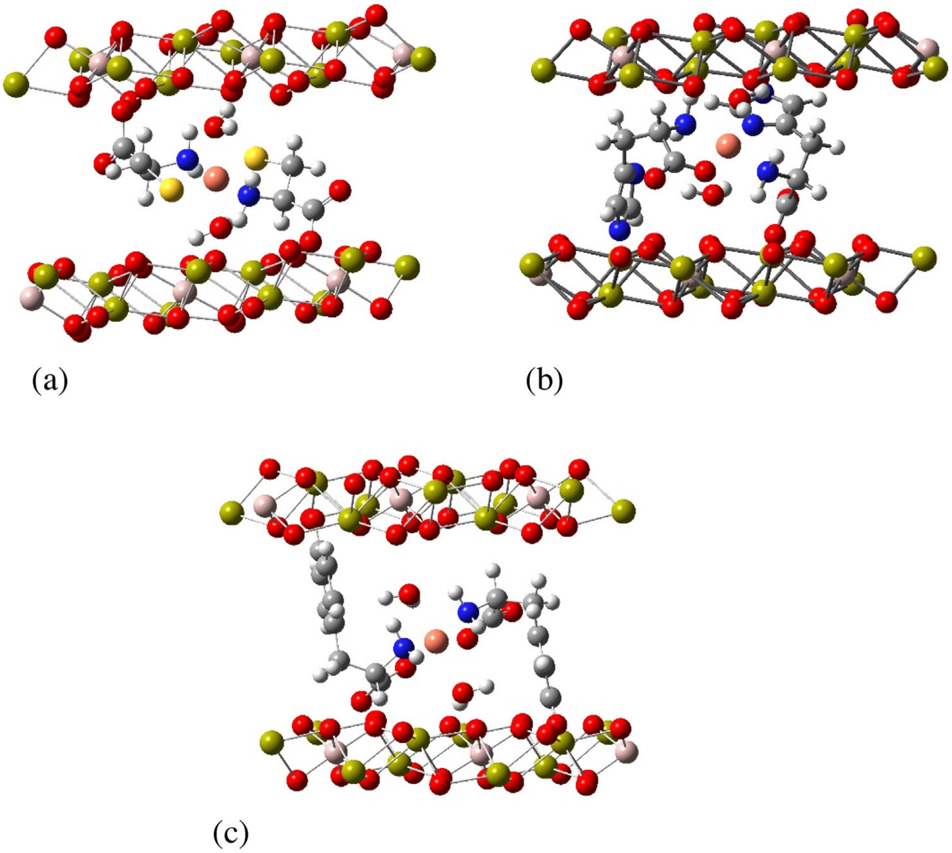

Fig. 15. The proposed steric arrangement of the intercalated complexes between the layers of CaAl-LDH, based on XRD, XAS, far IR and EPR measurements, (a) CaAl–Cu(II)-cysteinate–LDH, (b) Cu(II)-histidinate–CaAl-LDH, (c) Cu(II)-tyrosinate–CaAl-LDH.

Table 5
Conversions in three rounds of recycling in the oxidation of cyclohexene after 4 h (catalyst: 35 mg, acetone: 10 cm^3, cyclohexene: 5 mmol, peracetic acid: 2.5 mmol, temperature: 298 K, reactivation: rinsing with acetone).

Catalyst	Conversion (%)		
	1st Recycle	2nd Recycle	3rd Recycle
CaAl–Cu(II)-Cys–LDH	45	41	41
Cu(II)-His–CaAl-LDH	42	40	40
Cu(II)-Tyr–CaAl-LDH	49	48	41

hydrolysed *in situ*, in the solvent (aqueous acetone–5/95% by volume) according to the following equation [26]:

$$\mathrm{PhI(OOCH_3)_2 + H_2O \rightleftharpoons PhI(OH)_2 + 2CH_3COOH}$$

The TOF/conversion and selectivity values obtained with the *in situ* generated $\mathrm{PhI(OH)_2}$ are displayed in Table 6.

The added composites were real catalysts, since they largely retained their activities (Table 7) even in the third recycling experiments, and again, they were only rinsed with the solvent after each run as the regeneration step.

It is clear that the two oxidant–composite systems acted very differently.

On using peracetic acid as the oxidant neither the activities nor the selectivities changed significantly from composite to composite. This means that not the identity, but the presence of the ligands was important. Influencing the accessibility of the central ion was their major role. In the presence of the intercalated complex, direct coordination of the peracetic acid to the central ion may have occurred, replacing water molecule in the coordination sphere, and oxygen transfer to the double bond of the possibly uncoordinated cyclohexene could take place at this stage. This should be the reason of the outstanding epoxide selectivity. If both reactants were coordinated, there would be plenty of time for further reactions. If cyclohexene was coordinated alone, the situation would not be much different from the stoichiometric reaction.

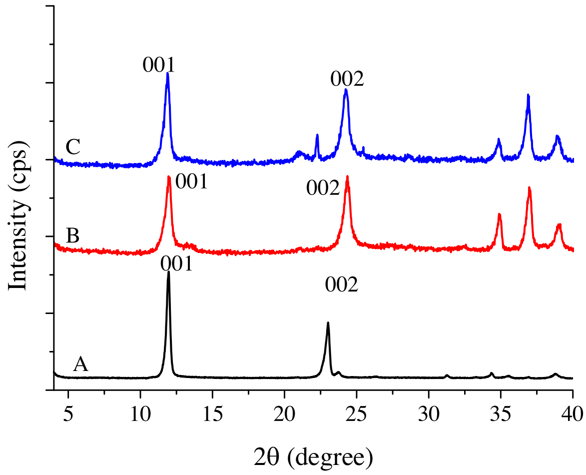

Fig. 16. X-ray diffractograms of Cu(II)-histidinate–CaAl-LDH after A: the 1st, B: the 2nd and C: the 3rd recycling.

The *cis* diol, in the second reaction, could not be formed *via* epoxide intermediate. Rather, the transfer of the two OH groups could have occurred in a concertic manner *via* a cyclic intermediate. This way, the *cis* configuration could be assured.

Table 6
The TOF/conversion and selectivity results of the oxidation of cyclohexene after 4 h (catalyst: 35 mg, aqueous acetone (5/95% by volume): 10 cm^3, cyclohexene: 5 mmol, (diacetoxyiodo)benzene acid: 2.5 mmol, temperature: 298 K).

Catalyst	TOF (1/h)/Conversion (%)	Epoxide (%)	2-Chex-1-ol (%)	2-Chex-1-one (%)	*Cis* diol (%)
–	nr/21	64	4	2	30
CaAl-LDH	nr/18	63	4	5	28
CaAl–Cu(II)-Cys–LDH	15.0/35	0	8	0	92
Cu(II)-His–CaAl-LDH	19.5/40	0	7	0	93
Cu(II)-Tyr–CaAl-LDH	11.6/41	0	0	0	100

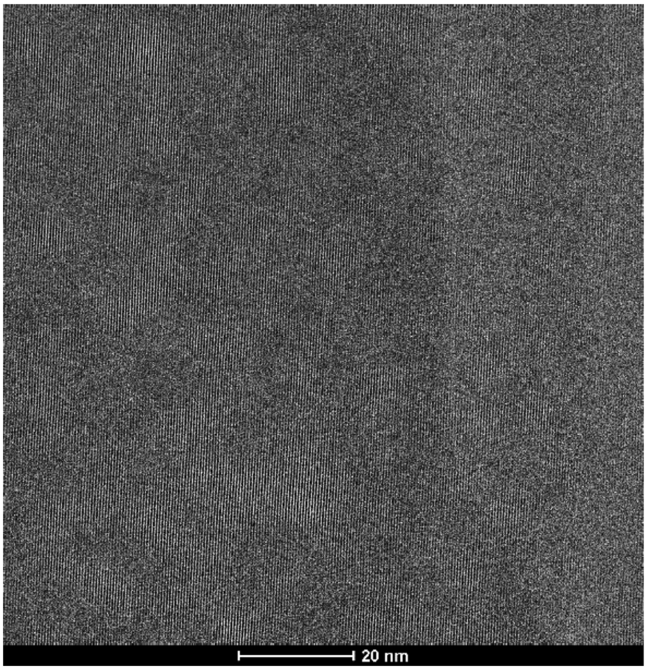

Fig. 17. TEM image Cu(II)-histidinate–CaAl-LDH after the 3rd recycling.

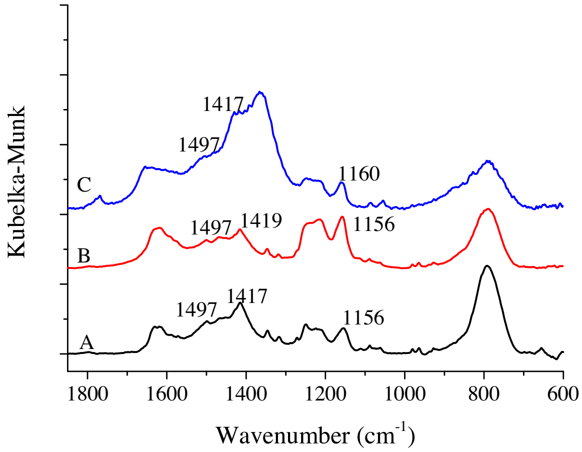

Fig. 18. FT-IR spectra of Cu(II)-histidinate–CaAl-LDH after A: the 1st, B: the 2nd and C: the 3rd recycling.

3.6.2. Structural features of the used composites

Possible structural changes of the used composites were studied with a variety of methods (TEM, XPS, XRD, IR). The example is Cu(II)-histidinate–CaAl-LDH, for the other two used composites, to reader is referred to the Supplementary Material (SFigs. 9–14).

The layered structure is retained even during recycling as is attested by the X-ray diffractograms (Fig. 16) and the TEM image taken after the third recycling (Fig. 17).

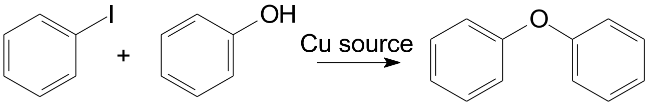

Scheme 2. The Ullmann diaryl etherification.

Table 7
Conversions in three rounds of recycling in the oxidation of cyclohexene after 4 h (catalyst: 35 mg, aqueous acetone (5/95% by volume): 10 cm^3, cyclohexene: 5 mmol, (diacetoxy-iodo)benzene: 2.5 mmol, temperature: 298 K, reactivation: rinsing with acetone).

Catalyst	Conversion (%)		
	1st Recycle	2nd Recycle	3rd Recycle
CaAl–Cu(II)-Cys–LDH	31	35	36
Cu(II)-His–CaAl-LDH	35	33	32
Cu(II)-Tyr–CaAl-LDH	36	37	31

Table 8
Conversion data of Ullmann reaction – the influence of the base (40 mg of catalyst, 5 cm^3 of toluene (when inorganic base was used, it was dissolved in 0.5 cm^3 of water), 0.6 mmol of iodobenzene, 0.5 mmol of phenol, 0.5 mmol of base, 24 h reaction time at 368 K).

Catalysts	Na_2CO_3	K_2CO_3	Piperidine	Added base-free
–	N/A	N/A	N/A	N/A
CaAl-LDH	N/A	3	N/A	3
CaAl–Cu(II)-Cys–LDH	23	65	54	21
Cu(II)-His–CaAl-LDH	30	73	50	27
Cu(II)-Tyr–CaAl-LDH	19	45	31	23

The organic material remained among the layers during the repeated reactions proven by the PA-IR spectra (Fig. 18). Copper, in the form of Cu^{2+} ions, is seen in the used catalyst in the X-ray photoelectron spectrum (Fig. 19).

The above figures reveal that the recycled composite did not undergo significant structural changes during the repeated reactions. Moreover, ICP measurement showed no copper ions in the reaction mixture after the repeated runs, *i.e.*, the composites served as heterogeneous catalysts (Scheme 2).

3.6.3. The Ullmann-type diaryl etherification as test reaction

The composites were actively catalysed the Ullmann reaction, too. It is to be noted that there was no reaction either without the LDH samples or in the presence of the pristine LDH. In this reaction, the presence of the added base is important, and K_2CO_3 proved to be the most efficient one. Higher conversion could be achieved over silica-supported Cu(I) or Cu(II) catalysts [27], but at significantly higher temperature (403 K) and in dimethyl formamide solvent, which cannot be used with LDHs because of its delaminating activity (Table 8).

The Ullmann diaryl etherification is a reaction known for a long time. It has been conducted under homogeneous or heterogeneous conditions, and much information has been collected (for a relatively recent review, see ref. [28].) Generally, the catalyst undergoes a Cu(I)–Cu(II)–Cu(I) redox cycle, but the Cu(II)–Cu(III)–Cu(II) redox cycle was also reported as feasible alternative [29]. In our system,

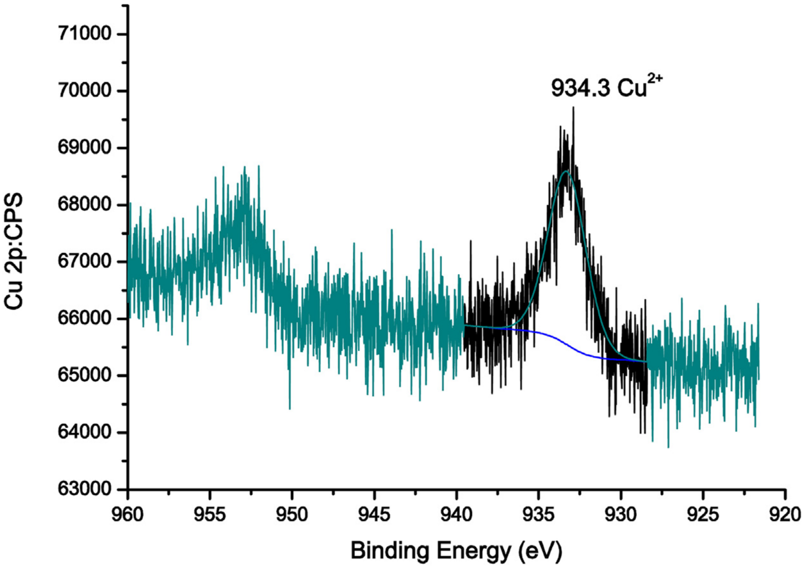

Fig. 19. XPS showing the Cu^{2+} ions of the used Cu(II)-histidinate–CaAl-LDH, after the 3rd recycling.

the former seems to be operational for the anchored complex with the cysteinate ligand [30], while the latter for the other two composites. Let us note that the reaction proceeded over the composites without added base, the LDH itself was basic enough to promote the coupling, although adding more base, especially of inorganic one, certainly improved the performance of the catalytic system.

4. Conclusions

Three composite materials having Cu(II)-amino acid complexes among the layers of CaAl-LDH were successfully synthesized either *via* sequential intercalation (introducing the ligands first, then constructing the complex–CaAl–Cu(II)-cysteinate–LDH) or direct intercalation of the preformed complex (Cu(II)-histidinate–CaAl-LDH and Cu(II)-tyrosinate–CaAl-LDH). The aim of having the complexes exclusively among the layers of the LDH was achieved, which was verified by using a range of instrumental methods (XRD, TEM, SEM, measurements, diffuse reflectance, ATR- and PA-IR spectroscopies).

The intercalant was also characterized by relevant, mostly instrumental methods (classical chemical and energy dispersive X-ray analysis, EPR, X-ray photoelectron, X-ray absorption and far IR spectroscopies) revealing a coordination number of six, and the imidazole nitrogen, the carboxylate group and the thiolate sulphur as sure coordination sites.

The intercalated substances were efficient, recyclable catalysts tested in the oxidation reactions of cyclohexene with two different oxidants giving two different products with very high selectivities (peracetic acid: epoxide, *in situ* formed iodosylbenzene: *cis*-diol). The catalysts also performed well in the Ullman etherification reaction.

Acknowledgment

This work was supported by the National Science Fund of Hungary through grant OTKA NKFI 106234. The financial help is highly appreciated.

Appendix A. Supplementary data

Supplementary data associated with this article can be found, in the online version, at http://dx.doi.org/10.1016/j.molcata.2016.06.008.

References

[1] S.J. Mills, A.G. Christy, J.M.R. Génin, T. Kameda, F. Colombo, Miner. Mag. 76 (2012) 1289–1336.
[2] Zs. Ferencz, M. Szabados, M. Ádok-Sipiczki, Á. Kukovecz, Z. Kónya, P. Sipos, I. Pálinkó, J. Mater. Sci. 49 (2014) 8478–8486.
[3] J. Qu, Q. Zhang, X. Li, X. He, S. Song, Appl. Clay Sci. 119 (2016) 185–192.
[4] Zs. Ferencz, M. Szabados, G. Varga, Z. Csendes, Á. Kukovecz, Z. Kónya, S. Carlson, P. Sipos, I. Pálinkó, J. Solid State Chem. 233 (2016) 236–243.
[5] M. Szabados, R. Mészáros, Sz. Erdei, Z. Kónya, Á. Kukovecz, P. Sipos, I. Pálinkó, Ultrason. Sonochem. 31 (2016) 409–416.
[6] V. Rives, M.A. Ulibarri, Coord. Chem. Rev. 181 (1999) 61–120.
[7] K.A. Carrado, J.E. Forman, R.E. Botto, R.E. Winans, Chem. Mater. 5 (1993) 472–478.
[8] B. Monteiro, S. Gago, S.S. Balula, A.A. Valente, I.S. Gonçalves, M. Pillinger, J. Catal. A 312 (2009) 23–30.
[9] M.-Z. Wang, Y. Li, J.-J. Ji, G.-L. Huang, X. Zhang, S.-H. Li, X.-J. Yang, Chin. Chem. Lett. 24 (2013) 593–596.
[10] G. Varga, Á. Kukovecz, Z. Kónya, L. Korecz, Sz. Muráth, Z. Csendes, G. Peintler, S. Carlson, P. Sipos, I. Pálinkó, J. Catal. 335 (2016) 125–134.
[11] G.N. George, I.F. Pickering, EXAFSPAK-A Suite of Computer Programs for Analysis of X-ray Absorption Spectra, Stanford Synchrotron Radiation Laboratory, Stanford, CA, 1995, http://www-ssrl.slac.stanford.edu/exafspak.html (accessed January, 2016).
[12] A. Rockenbauer, L. Korecz, Appl. Magn. Res. 10 (1996) 29–43.
[13] F. Ullmann, P. Sponagel, Chem. Ber. 38 (1905) 2211–2212.
[14] B. Evertsson, Acta Crystallogr. Sect. B 25 (1969) 30–41.
[15] A. Manceau, A. Matynia, Geochim. Cosmochim. Acta 74 (2010) 2256–2580.
[16] G. Varga, Z. Csendes, G. Peintler, O. Berkesi, P. Sipos, I. Pálinkó, Spectrochim. Acta A 122 (2014) 257–259.
[17] G.G. Mohamed, M.M. Omar, A.A. Ibrahim, Eur. J. Med. Chem. 44 (2009) 4801–4812.
[18] K. Várnagy, E. Garribba, D. Sanna, I. Sóvágó, G. Micera, Polyhedron 24 (2005) 799–806.
[19] T. Szabó-Plánka, A. Rockenbauer, L. Korecz, D. Nagy, Polyhedron 19 (2000) 1123–1131.
[20] L.D. Pinto, P.A.L. Puppin, V.M. Behring, O.C. Alves, N.A. Rey, J. Felcman, Inorg. Chim. Acta 386 (2012) 60–67.
[21] J.A. Farrar, A. Formicka, M. Zeppezauer, A.J. Thomson, J. Biochem. 317 (1996) 447–456.
[22] M. Sacerdoti, E. Passaglia, Neues Jahrbuch für Mineralogie, Monatshefte 1988, Hydrocalumite from Latium, Italy: its crystal structure and relationship with related phases, pp. 462–475.
[23] M. Shokouhimehr, K.-Y. Shin, J.S. Lee, M.J. Hackett, S.W. Jun, M.H. Oh, J. Jang, T. Hyeon, J. Mater. Chem. A 2 (2014) 7593–7599.

[24] M. Shokouhimehr, Y. Piao, J. Kim, Y. Jang, T. Hyeon, Angew. Chem. Int. Ed. 46 (2007) 7039–7043.
[25] D.E. de Vos, B.F. Sels, P.A. Jacobs, Cattech 6 (2002) 14–29.
[26] J.-H. In, S.-E. Park, R. Song, W. Nam, Inorg. Chim. Acta 343 (2003) 373–376.
[27] T. Miao, L. Wang, Tetrahedron Lett. 48 (2007) 95–99.
[28] F. Monnier, M. Taillefer, Angew. Chem. Int. Ed. 48 (2009) 6954–6971.
[29] I.P. Beletskaya, A.V. Cheprakov, Coord. Chem. Rev. 248 (2004) 2337–2364.
[30] L. Pecci, G. Montefoschi, G. Musci, D. Cavallini, Amino Acids 13 (1997) 355–367.